



POLİTEKNİK DERGİSİ

*JOURNAL of POLYTECHNIC*

ISSN: 1302-0900 (PRINT), ISSN: 2147-9429 (ONLINE)

URL: <http://dergipark.gov.tr/politeknik>



# Investigation of nonlinear behavior of the reinforced concrete columns for different confined concrete models

*Farklı sarılı beton modelleri için betonarme kolonların doğrusal olmayan davranışlarının incelenmesi*

*Authors (Yazarlar): Saeid Foroughi <sup>1</sup>, S. Bahadır Yüksel <sup>2</sup>*

ORCID<sup>1</sup>: 0000-0002-7556-2118

ORCID<sup>2</sup>: 0000-0002-4175-1156

**Bu makaleye şu şekilde atıfta bulunabilirsiniz (To cite to this article):** Foroughi S. ve Yüksel S. B., "Investigation of nonlinear behavior of the reinforced concrete columns for different confined concrete models", *Politeknik Dergisi*, 25(4): 1447-1462, (2022).

**Erişim linki (To link to this article):** <http://dergipark.gov.tr/politeknik/archive>

**DOI:** 10.2339/politeknik.930774

# Investigation of Nonlinear Behavior of the Reinforced Concrete Columns for Different Confined Concrete Models

## Highlights

- ❖ Nonlinear behavior, stress-strain and moment-curvature
- ❖ Confined concrete strength and lateral confining stress

## Graphical Abstract

Stress-strain and moment-curvature behavior of the reinforced concrete (RC) square columns have been analytically investigated according to different confined concrete models.

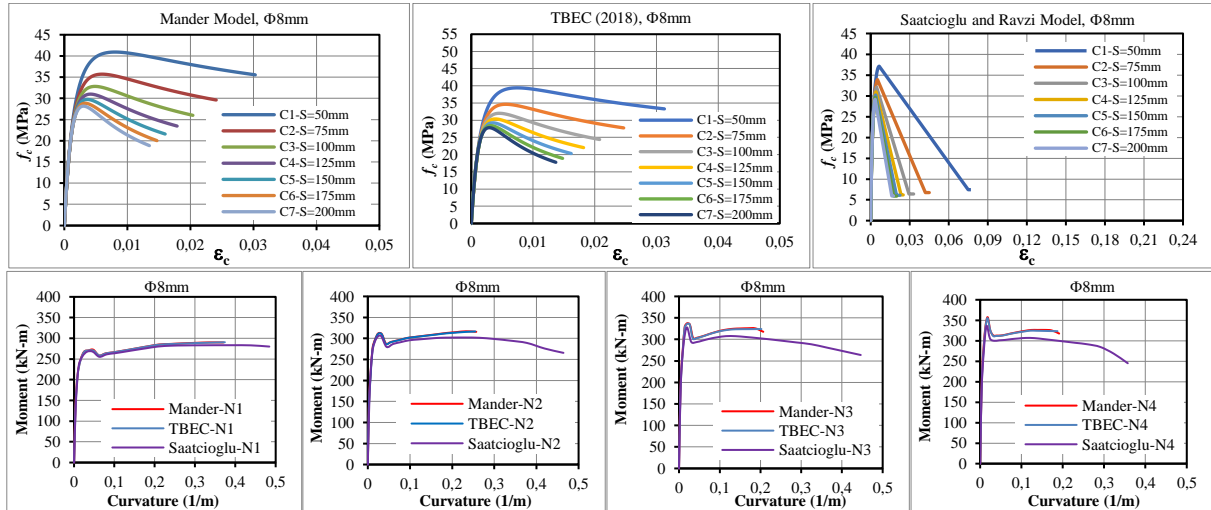


Figure. Stress-strain and moment-curvature relationships for reinforced concrete columns

## Aim

Investigations of the effect of transverse reinforcement ratio and axial load on the behavior of the reinforced concrete square columns are the main purpose of this study.

## Design & Methodology

To better understand the non-linear behavior, information was provided about stress-strain behavior models recommended by the TBEC (2018), Mander et al., (1988), Saatcioglu and Ravzi (1992). Using the proposed models of confined concrete compressive strength of the RC column models were investigated analytically.

## Originality

The literature on the confined concrete models has been reviewed and the stress-strain and moment-curvature relationships of reinforced concrete elements have been calculated according to the current TBDY (2018) regulation. Comparison of the nonlinear behaviors obtained from the TBDY (2018) and the confined concrete models found in the literature has been a current study on behalf of the literature.

## Findings

The greatest ultimate curvature values were calculated from the Saatcioglu and Ravzi models (average 24%). In the examination of ultimate curvature values obtained according to the Mander model and TBEC, there is not much difference. There is a negligible difference between the ultimate moment values obtained according to the Mander model and TBEC. It is seen from the results of the analysis that there is not much difference between the stress and strain values obtained for these two models. According to Mander, Saatcioglu and Ravzi models, the average difference value is 3.1% between the ultimate moment values.

## Conclusion

As a result, it has been observed that when the close to minimum and minimum spacing value, high confined concrete strength values and the ultimate moment values are obtained from the Mander model than Saatcioglu and Ravzi model. These differences are not much between the Mander model and TBEC (2018).

## Declaration of Ethical Standards

The authors of this article declares that the materials and methods used in this study do not require an ethical committee permission and/or legal-special permission

# Investigation of Nonlinear Behavior of the Reinforced Concrete Columns for Different Confined Concrete Models

*Araştırma Makalesi / Research Article*

**Saeid Foroughi<sup>\*</sup>, S. Bahadır Yüksel**

Konya Technical University, Department of Civil Engineering, Faculty of Engineering and Natural Sciences, Konya, Turkey

(Geliş/Received : 01.05.2021 ; Kabul/Accepted : 03.06.2021 ; Erken Görünüm/Early View : 10.06.2021)

## ABSTRACT

Stress-strain and moment-curvature behavior of the reinforced concrete (RC) square columns have been analytically investigated according to different confined concrete models. The effect of transverse reinforcement diameter, transverse reinforcement spacing and concrete grade on the behavior of RC column models were investigated. For different confined concrete models, the confinement effectiveness coefficient, effective lateral confining stress, confined concrete compressive strength, strain at maximum concrete stress and ultimate concrete compressive strain values were calculated. In the second part, a parametric investigation was carried out for examining the effects of different design parameters on the moment-curvature relationships. Analytical moment-curvature relationships were obtained for RC cross-sections by using the TBEC (2018), Mander model (1988), Saatcioglu and Ravzi (1992) confined concrete models. The effects of the design parameters on the RC square column behavior were evaluated in terms of moment capacity and the curvature of the cross-section. In RC column models, stress-strain and moment-curvature relationships are obtained and compared according to different parameters. Confined concrete strength and the ultimate moment values obtained from the Mander model were higher than the Saatcioglu and Ravzi model when the transverse reinforcement close to the minimum spacing values. The results obtained from the Mander model and TBEC (2018) are close to each other.

**Keywords:** Stress-strain, moment-curvature, nonlinear behavior, confined concrete strength, lateral confining stress.

## Farklı Sarılı Beton Modelleri için Betonarme Kolonların Doğrusal Olmayan Davranışlarının İncelenmesi

### ÖZ

Betonarme kare kolonların farklı sargılı beton modellerine göre gerilme-şekil değiştirme ve moment-eğrilik davranışı analitik olarak incelenmiştir. Enine donatı oranı ve beton sınıfının betonarme kolon modellerinin davranışına etkisi incelenmiştir. Farklı sargılı beton modelleri için sargı etkinlik katsayısı, etkili yanal basınç gerilmesi, sargılı beton basınç dayanımı, maksimum beton gerilmesinde birim kısalma ve sargılı betondaki maksimum basınç birim şekil değiştirme değerleri hesaplanmıştır. İkinci bölümde, farklı tasarım parametrelerinin moment-eğrilik ilişkileri üzerindeki etkilerinin incelenmesi için parametrik bir araştırma yapılmıştır. TBDY (2018), Mander modeli (1988), Saatcioglu ve Ravzi (1992) sargılı beton modelleri kullanılarak betonarme kesitlerde analitik moment-eğrilik ilişkileri elde edilmiştir. Parametrelerin betonarme kare kolon davranışı üzerindeki etkileri, enine kesitin eğrilik ve moment kapasitesi açısından değerlendirilmiştir. Betonarme kolon modellerinde, gerilme-şekil değiştirme ve moment-eğrilik ilişkileri elde edilmiş ve farklı parametrelere göre karşılaştırılmıştır. Mander modelinden elde edilen sargılı beton basınç dayanımı ve nihai moment değerleri, enine donatı minimum aralık değerlerine yakın olduğunda Saatcioglu ve Ravzi modeline göre daha yüksektir. Mander modelinden ve TBDY (2018) ile elde edilen sonuçlar birbirine yakındır.

**Anahtar Kelimeler:** Gerilme-şekil değiştirme, moment-eğrilik, doğrusal olmayan davranış, sargılı beton dayanımı, yanal sargı basıncı.

### 1. INTRODUCTION

Understanding the nonlinear response and damage characteristics of buildings subjected to significant earthquakes is essential for the assessment of the seismic performance of existing buildings, as well as the safe and economic design of new buildings [1]. Reinforced concrete (RC) columns are the critical members of moment-resisting structural systems and have to be

designed adequately in strength and ductility [2]. Usually, it is desirable to design a RC member with sufficient curvature ductility capacity to avoid brittle failure in flexure and to insure ductile behavior, especially under seismic conditions [3]. The correct estimate of curvature ductility of reinforced concrete members has always been an attractive subject of study as it engenders a reliable estimate of the capacity of buildings under seismic loads [4]. In order to see the real behavior of a reinforced concrete cross-section, a concrete model that takes the transverse reinforcement

*\*Sorumlu Yazar (Corresponding Author)*  
e-posta : saeid.foroughi@yahoo.com

ratio into consideration should be used [5]. The load-bearing capacity of reinforced concrete column sections ends with the destruction of the core concrete [6]. Theoretical moment-curvature analysis for RC structural elements indicating the available flexural strength and ductility can be constructed providing that the stress-strain relations for both concrete and steel are known [7]. In seismically active areas, the ductility of structures is an important parameter for structural design [8]. The moment-curvature relationship is one of the best solutions to evaluate and represent the behavior of RC cross-sections [9].

Realistic moment-curvature relationships can only be obtained if realistic material constitutive models are utilized for confined and unconfined concrete and reinforcing steel during the cross-sectional moment-curvature analysis [10]. In order to achieve a more accurate simulation of the real structural behavior, designers need the accurate stress-strain relationships for unconfined and confined concrete [11]. The stress-strain curve of concrete under compression, and in particular the compressive strength, ultimate strain and post-peak branch, have an important role in the design of concrete and concrete-based structures [12]. Ductile and durable concrete structures are the goal of all designers. In order to achieve such goals, it is necessary to know the laws that govern the behavior of materials and structures for both nonlinearities: the geometrically nonlinear effects and nonlinear behavior of the material caused by inelastic deformation [13]. Good modeling of the axial compressive stress-strain behavior of confined RC columns is necessary for the structural analysis and design to assess their strength and ductility capacities [14-15]. It is well known that the strength and ductility of concrete are highly dependent on the level of confinement provided by the lateral reinforcement. [16-17]. In the literature, a large number of stress-strain relationship models were proposed for confined and unconfined concrete. The factors that are generally taken into consideration in these models are the amount of transverse reinforcement, concrete and reinforcement strength, distribution of longitudinal and transverse reinforcement in cross-section, transverse reinforcement spacing and cross-section dimensions. To better understand the non-linear behavior, information was provided about stress-strain behavior models recommended by the Turkish Building Earthquake Code (TBEC) [18], Mander et al. [19], Saatcioglu and Ravzi [20]. Using the proposed models of TBEC [18], Mander et al. [19], Saatcioglu and Ravzi [20] the confined concrete compressive strength of the RC column models were investigated analytically. A total of 105 column models with different parameters were designed. The effect of changing the concrete grade and transverse reinforcement ratio on the behavior of RC sections was examined according to TBEC [18], Mander et al. [19], Saatcioglu and Ravzi [20] models. The stress-strain curves were obtained for various models and were interpreted by comparing the curves. In the second part,

a parametric investigation was carried out to be able to examine the effects of various variables on the moment-curvature relationships, such as concrete grade, axial load level, transverse reinforcement diameter and spacing. Analytical moment-curvature relationships were obtained for RC column models by using different confined concrete models. The examined behavioral effects of the parameters were evaluated by the curvature ductility and the cross-section strength. The stress-strain curves and moment-curvature curves were drawn for various models and were interpreted by comparing the curves.

## 2. STRESS-STRAIN RELATIONSHIP

### 2.1. Theoretical Stress-Strain for Mander Model [19]

Thus, the effect of confinement on the strength and deformation capacity of concrete members has been extensively studied [2, 22]. Many mathematical models for the confined concrete are currently used in the analysis of RC structures [23-24]. Mander et al. [19] have proposed a unified stress-strain approach for confined concrete applicable to both circular and rectangular shaped transverse reinforcement. The stress-strain model is illustrated in Fig. 1a. and is based on an Equation suggested by Popovics [25].

The confinement effectiveness coefficient ( $k_e$ ) represents the ratio of the smallest effectively confined concrete area ( $A_e$ ) to the confined concrete core area ( $A_{cc}$ ) (Eq. 1). Where  $\rho_{cc}$  is ratio of area of longitudinal reinforcement to area of concrete core,  $S'$  clear vertical spacing between hoops,  $b_c$  and  $d_c$  is the concrete core dimension to center-line of perimeter hoop in  $x$  and  $y$  direction,  $w'_i$  clear transverse spacing between adjacent longitudinal bars (Fig. 1b).

$$k_e = \left( 1 - \sum_i^n \frac{(w'_i)^2}{6} \right) \left( 1 - \frac{S'}{2b_c} \right) \left( 1 - \frac{S'}{2d_c} \right) / (1 - \rho_{cc}) \quad (1)$$

Effective lateral confining stresses in the  $x$  and  $y$  directions and effective lateral confining pressure are given in Eq. (2).

$$f'_{lx} = k_e \frac{A_{sx}}{S.d_c} f_{yh}, \quad f'_{ly} = k_e \frac{A_{sy}}{S.b_c} f_{yh}, \quad f'_l = \frac{f'_{lx} + f'_{ly}}{2} \quad (2)$$

To determine the confined concrete compressive strength  $f'_{cc}$ ;

$$f'_{cc} = f'_{co} \left( -1.254 + 2.254 \sqrt{1 + \frac{7.94 f'_l}{f'_{co}}} - 2 \frac{f'_l}{f'_{co}} \right) \quad (3)$$

The longitudinal concrete stress ( $f_c$ ) is given as the function of the longitudinal concrete strain ( $\epsilon_c$ ). In Eq. (4),  $f_c$  and  $\epsilon_c$  represent the concrete strength and the corresponding strain value, respectively. is compressive

strength of confined concrete and  $\epsilon_c$  is the longitudinal compressive concrete strain.

$$f_c = \frac{f'_{cc} \cdot x \cdot r}{r - 1 + x^r}, \quad x = \frac{\epsilon_c}{\epsilon_{cc}}, \quad r = \frac{E_c}{E_c - E_{sec}} \quad (4)$$

$$E_c = 5000\sqrt{f'_{co}} \text{ MPa}, \quad E_{sec} = \frac{f'_{cc}}{\epsilon_{cc}}$$

The corresponding strain at maximum concrete stress ( $\epsilon_{cc}$ ) and maximum concrete compressive strain ( $\epsilon_{cu}$ ) for confined concrete has to be calculated too (Eq. 5).  $f'_{co}$  and  $\epsilon_{co}$  represent the unconfined concrete strength and corresponding strain, respectively ( $\epsilon_{co} = 0.002$ ).

$$\epsilon_{cc} = \epsilon_{co} \left[ 1 + 5 \left( \frac{f'_{cc}}{f'_{co}} - 1 \right) \right], \quad \epsilon_{cu} = 0.004 + \frac{1.4 \rho_s f_{yw} \epsilon_{su}}{f'_{cc}} \quad (5)$$

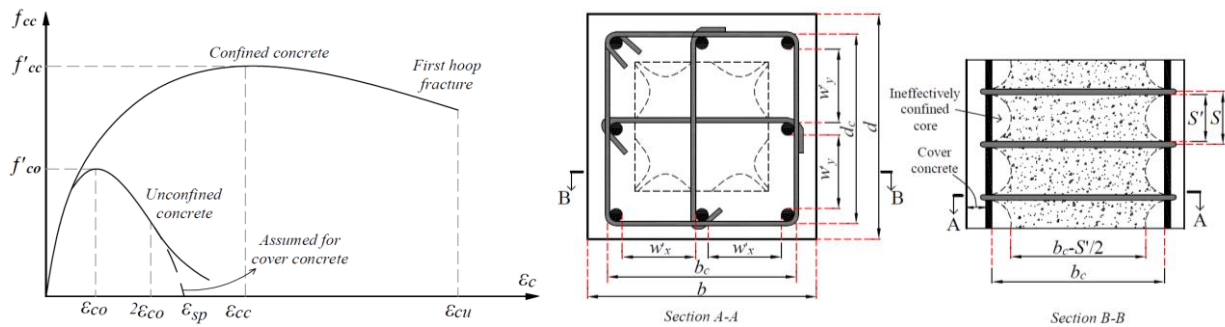


**Figure 1.** a) Stress-strain model proposed for unconfined and confined concrete, b) Effectively confined core for transverse reinforcement [19]

**2.2. TBEC [18] Confined Concrete Models**

In the evaluation according to strain by nonlinear methods, the following stress-strain relations are defined for confined and unconfined concrete to be used when no other model is selected. The stress-strain relationship for materials given in TBEC [18] were used (Fig. 2).

$$f_{cc} = \lambda_c \cdot f_{co} = f_{co} \left( -1.254 + 2.254 \sqrt{1 + 7.94 \frac{f_e}{f_{co}}} - 2 \frac{f_e}{f_{co}} \right) \quad (6)$$

Relation between confined concrete strength  $f_{cc}$  and unconfined concrete strength  $f_{co}$  in this correlation is given below.  $f_e$  effective confined pressure in here, can be taken as the average of values given below for the two perpendicular directions in rectangular sections:

$$f_{ex} = k_e \rho_x f_{yw}, \quad f_{ey} = k_e \rho_y f_{yw} \quad (7)$$

$f_{yw}$  yield stress of the transverse reinforcement indicates the volumetric ratios of transverse reinforcements in  $\rho_x$  and  $\rho_y$  relevant directions whereas  $k_e$  indicates confined performance factor as defined in Eq. (8).

$$k_e = \left( 1 - \frac{\sum a_i^2}{6b_o h_o} \right) \left( 1 - \frac{S}{2b_o} \right) \left( 1 - \frac{S}{2h_o} \right) \left( 1 - \frac{A_s}{b_o h_o} \right)^{-1} \quad (8)$$

Here  $a_i$  indicates the distance between the axes of longitudinal reinforcements in the periphery of section,  $b_o$  and  $h_o$  indicates the section sizes remain among the axes of hoops that confined the core concrete,  $s$  indicates the distance between the axes of transverse reinforcement in vertical direction,  $A_s$  indicates area of longitudinal reinforcement (Fig. 3). Concrete compressive stress in confined concrete ( $f_c$ ), is given with the Eq. (4) correlation as the function of compressive unit deformation ( $\epsilon_{cc}$ ).

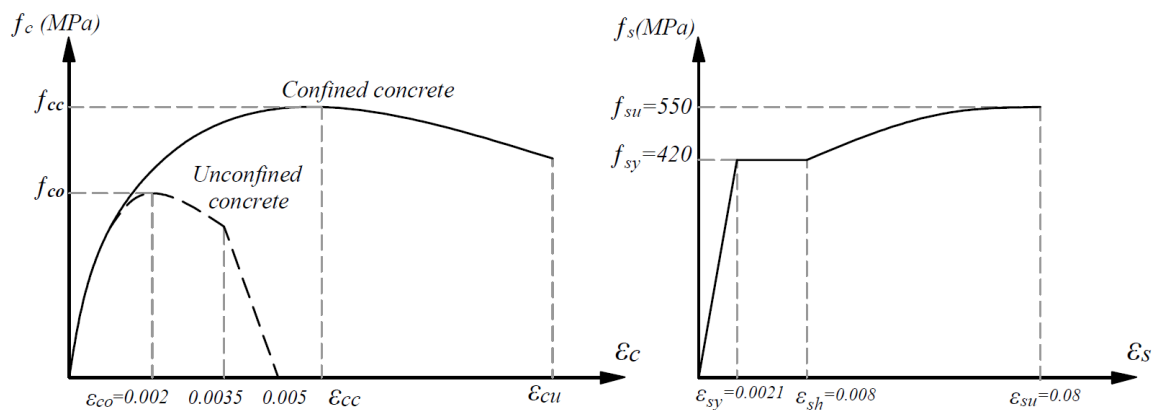


**Figure 2.** Stress-strain relationship for concrete and reinforcement [18]

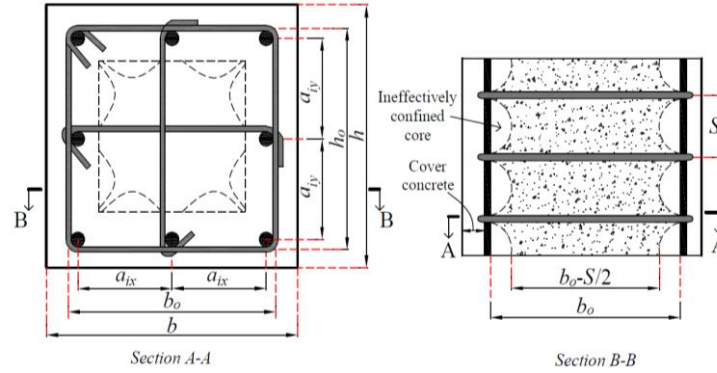


Figure 3. Effectively confined core for transverse reinforcement [18]

**2.3. Theoretical Stress-Strain for Saatcioglu and Ravzi model [20]**

An analytical model is proposed to construct a stress-strain relation and Effectively confined core for transverse reinforcement (Fig. 4). This developed model is directly formed by a rising parabolic arm, a linearly falling arm up to %20 of the strength, and a stable continuation after that point. Considering the effect of lateral confining stress  $\sigma_2$ , the confined concrete strength is obtained from Eq. (9).  $f'_{cc}$  and  $f'_{co}$  is the confined and unconfined strengths of concrete, respectively. For normal concrete strength,  $k_3=0.85$  is generally assumed. The expression given herein, obtained from regression analysis of test data, reflects the variation of coefficient  $k_1$  with lateral pressure.

$$f_{cc} = k_3 f_c + k_1 \sigma_{2e}, \quad k_1 = \frac{6.7}{(\sigma_{2e})^{0.17}} \quad (9)$$

Using the experimental data,  $\sigma_{2e}$  is derived from the Eq. (10). The variation of coefficient  $k_1$  with lateral pressure  $\sigma_{2e}$  was obtained from experimental data [20]. The equivalent uniform pressure  $\sigma_{2e}$  was established by reducing the average pressure with due considerations given to the appropriate parameters. Therefore, coefficient  $\beta$  was introduced to reduce the average pressure. The following expression, also used by previous researchers [19] is found to produce good predictions of experimentally obtained strain values corresponding to peak stress ( $\epsilon_{co}=0.002$ ).

$$\sigma_{2e} = \beta \sigma_2, \quad \sigma_2 = \frac{\sum A_o f_{yw} (\sin a)}{(s \times b_k)} \quad (10)$$

$$\beta = 0.26 \sqrt{\left(\frac{b_k}{a}\right) \left(\frac{b_k}{s}\right) \left(\frac{1}{\sigma_2}\right)} \leq 1$$

$$\epsilon_{coc} = \epsilon_{co} (1 + 5\lambda), \quad \lambda = \frac{k_1 \sigma_{2e}}{k_3 f_c} \quad (11)$$

Eq. (12) can be used to establish the strain at %85 strength levels beyond the peak. In the absence of test data, a value of 0.0038 may be appropriate for  $\epsilon_{u85}$ , under slow rate of loading. The total area of transverse reinforcement in two directions, crossing  $b_{kx}$  and  $b_{ky}$  can be calculated by Eq. (13).

$$\epsilon_{c85} = 260 \rho \epsilon_{coc} + \epsilon_{u85} \quad (12)$$

$$\rho = \frac{\sum A_{oxy} \sin a}{s(b_{kx} + b_{ky})} \quad (13)$$

Eq. (14) is suggested for the parabolic ascending portion and linear portion for the descending branch. The first and the second part of the curve:

$$\sigma_c = f_{cc} \left[ \left( \frac{2\epsilon_c}{\epsilon_{coc}} \right) - \left( \frac{\epsilon_c}{\epsilon_{coc}} \right)^2 \right]^{\frac{1}{1+2\lambda}} \leq f_{cc} \quad (14)$$

$$\sigma_c = f_{cc} + \left( \frac{f_{cc} - f_{c85}}{\epsilon_{coc} - \epsilon_{c85}} \right) (\epsilon_c - \epsilon_{coc})$$

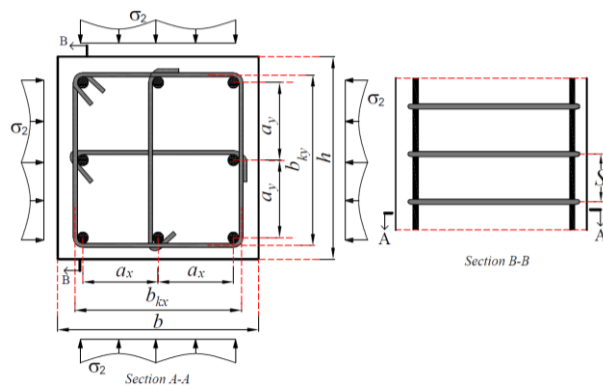
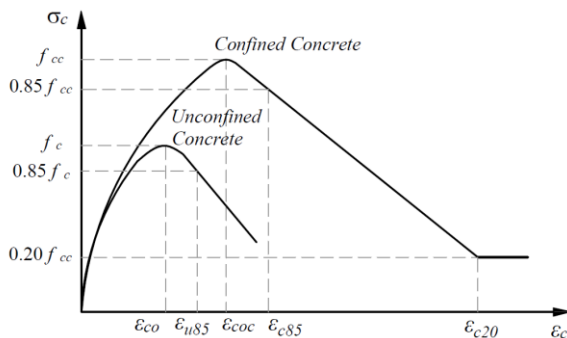


Figure 4. a) Proposed stress-strain relationship by Saatcioglu and Ravzi b) Effectively confined core for transverse reinforcement [20]

### 3. MOMENT-CURVATURE RELATION

Investigations of the effect of transverse reinforcement ratio and axial load on the behavior of the RC square columns are the main purpose of this study. The moment-curvature relationships of the RC columns having different axial load levels have been obtained by considering the different concrete models [18-20]. The combined effect of vertical and seismic loads ( $N_{dm}$ ), the cross-section area of the column shall satisfy the condition  $A_c \geq N_{dmax}/0.40f_{ck}$  [18]. In this section, the moment-curvature relationships of the column sections were investigated for the values of  $N/N_{max}$  ratios of 0.10, 0.20, 0.30 and 0.40. Moment-curvature relationships were obtained by SAP2000 Software [21]. In this part of the study, the moment-curvature relations are obtained by changing the concrete grade, axial load level, transverse reinforcement diameter and spacing.

### 4. MATERIAL AND METHOD

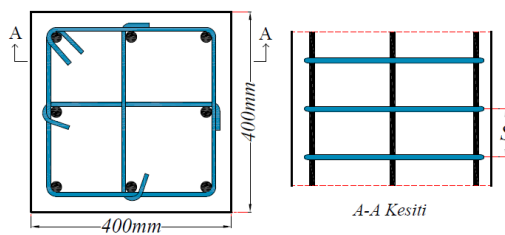
RC columns having square cross sections were designed considering the regulations of ACI318 [26] and TBEC [18]. The column models having dimensions of 400mm×400mm square cross sections were designed

(Table 1). Different transverse reinforcement diameters;  $\Phi 8$ mm,  $\Phi 10$ mm and  $\Phi 12$ mm and the transverse reinforcement spacing; 50mm, 75mm, 100mm, 125mm, 150mm, 175mm and 200mm were selected in order to investigate the effect of the transverse reinforcement on the cross-section behavior. In all the models the longitudinal column reinforcement was  $8\Phi 22$ mm. For all RC square column models, C30, C35, C40, C45 and C50 was chosen as concrete grade and B420C was selected as reinforcement for the reinforcement behavior model. The stress-strain relationship for materials given in TBEC [18] were used. For the recommended confined concrete models [18-20], the confinement effectiveness coefficient, effective lateral confining stress, confined concrete compressive strength, strain at maximum concrete stress and ultimate concrete compressive strain values were calculated. Stress-strain relations were obtained by calculating the values of confined concrete strength and confined concrete strain for the designed concrete models. Theoretical moment-curvature analysis for RC columns indicating the available bending moment and ductility can be constructed providing that the stress-strain relations for both concrete and steel models are known.

**Table 1.** Details for the designed model cross-sections

Material	No	Transverse Reinforcement	No	Transverse Reinforcement	No	Transverse Reinforcement
C30	C1	$\Phi 8/50$ mm	C8	$\Phi 10/50$ mm	C15	$\Phi 12/50$ mm
	C2	$\Phi 8/75$ mm	C9	$\Phi 10/75$ mm	C16	$\Phi 12/75$ mm
C35	C3	$\Phi 8/100$ mm	C10	$\Phi 10/100$ mm	C17	$\Phi 12/100$ mm
C40	C4	$\Phi 8/125$ mm	C11	$\Phi 10/125$ mm	C18	$\Phi 12/125$ mm
C45	C5	$\Phi 8/150$ mm	C12	$\Phi 10/150$ mm	C19	$\Phi 12/150$ mm
C50	C6	$\Phi 8/175$ mm	C13	$\Phi 10/175$ mm	C20	$\Phi 12/175$ mm
	C7	$\Phi 8/200$ mm	C14	$\Phi 10/200$ mm	C21	$\Phi 12/200$ mm

Cross-Section Dimention



### 5. NUMERICAL STUDY

The inelastic behavior of RC square column models was investigated using the stress-strain and moment-curvature relationships obtained based on real material behaviors. Confined concrete strengths were calculated according to the different concrete models [18-20] and the stress-strain results were obtained and compared. Stress-strain relationships of the confined core regions inside the RC columns (C1 to C21) for the different concrete grade, transverse reinforcement diameters and transverse reinforcement spacing were defined analytically. Theoretical moment-curvature analysis for

RC columns indicating the available bending moment and ductility can be constructed providing that the stress-strain relations for both concrete and steel are known. The moment-curvature relationships obtained from the analytical results are presented in graphical form.

#### 5.1. Stress-Strain Relationships According to The Mander Model

The obtained stress-strain relationship of the concrete stress ( $f_c$ ) as function of the concrete strain ( $\epsilon_c$ ) is summarized in Fig. 4. according to Mander et al. [19] model.

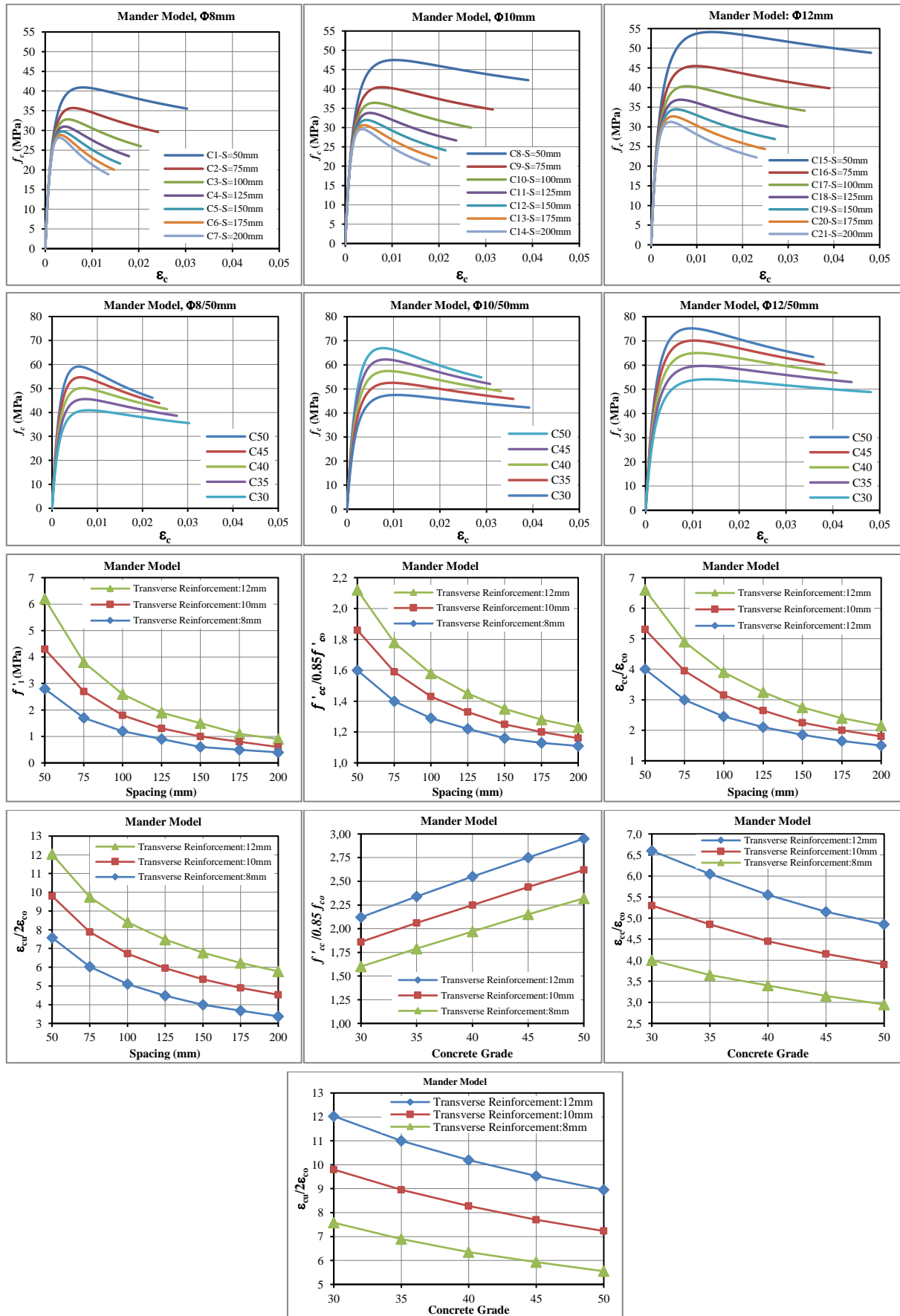


Figure 4. Stress-strain relationships of the RC columns for the different parameters.

**5.2. Stress-strain relationships according to the Saatcioglu and Ravzi model**

The confined concrete strength was calculated by using Saatcioglu and Ravzi concrete model [20] for the

designed column cross sections. The obtained stress-strain relationship of the concrete stress ( $f_c$ ) as functions of the concrete strain ( $\epsilon_c$ ) is summarized in Fig. 5. for Saatcioglu and Ravzi concrete model

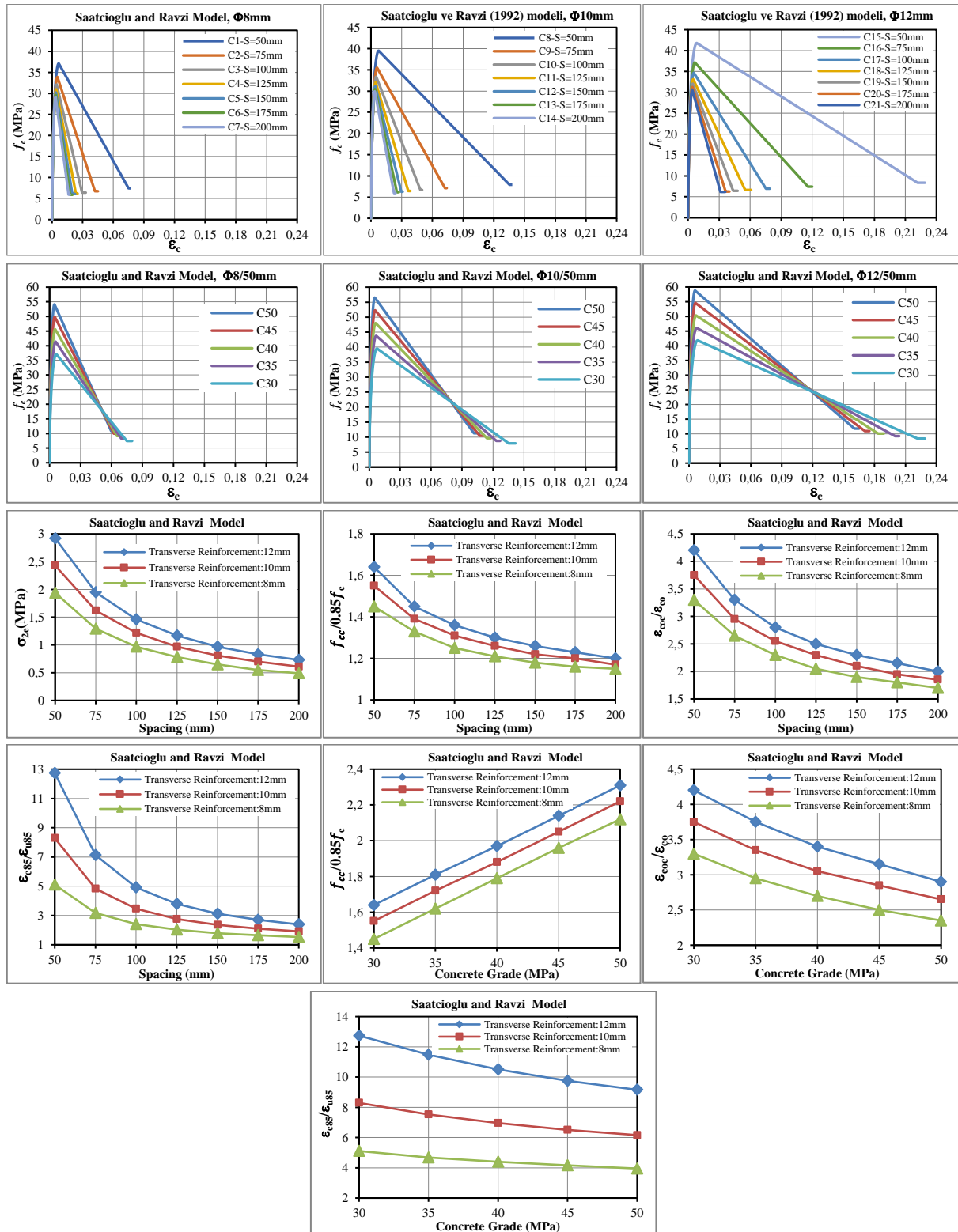


Figure 5. Stress-strain relationships of the RC columns for the different parameters.

### 5.3. Stress-strain relationships according to the TBEC

The confined concrete strength was calculated by the TBEC [18] for the designed column cross sections. The

obtained stress-strain relationship of the concrete stress ( $f_c$ ) as functions of the concrete strain ( $\epsilon_c$ ) is summarized in Fig. 6. according to TBEC [18].

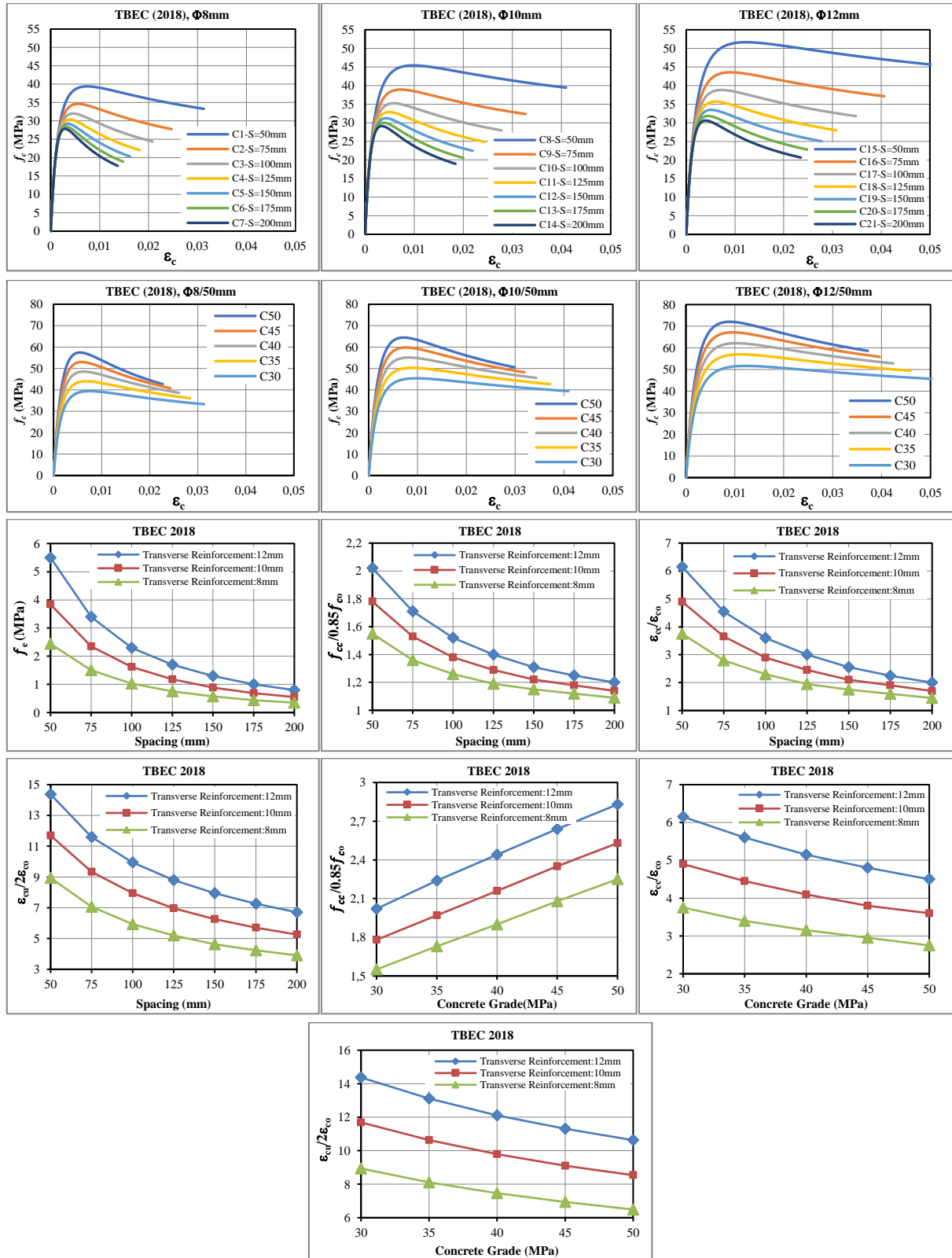


Figure 6. Stress-strain relationships of the RC columns for the different parameters.

### 5.4. Moment-Curvature Relationship of Square Columns

Moment-curvature relationships of square columns for different transverse reinforcement spacing and axial load levels were obtained. The moment-curvature relationships obtained from the analytical results are

presented in graphical form. Fig. 7. and Fig. 8. show the moment-curvature relationships for confined concrete models [18-20]. Moment-curvature relationships for different transverse reinforcement diameters and axial load levels are shown in Fig. 9.

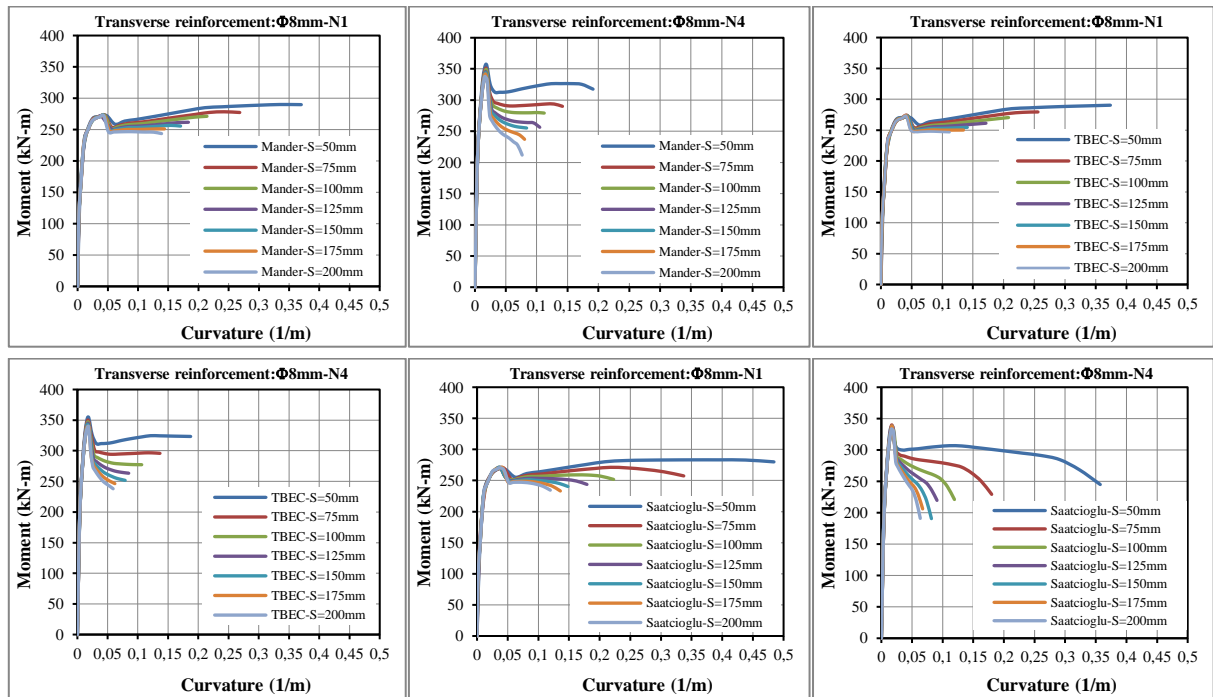


Figure 7. Moment-curvature relationships for different transverse reinforcement spacing and axial load levels.

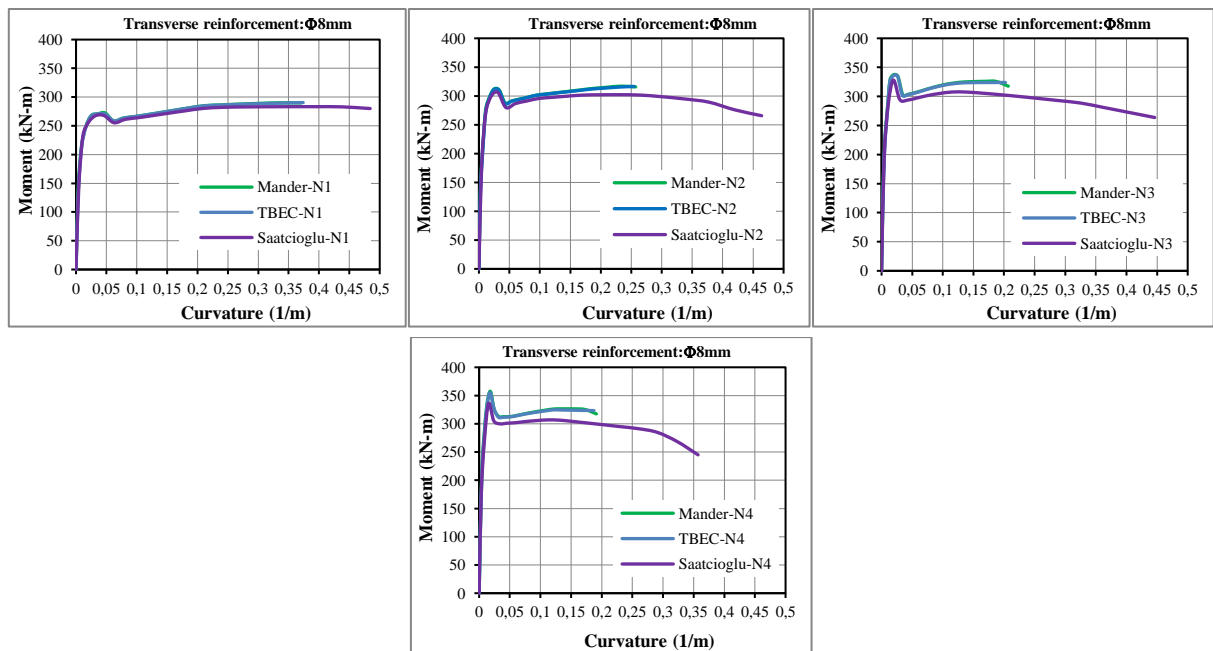


Figure 8. Moment-curvature relationships for different confined concrete models

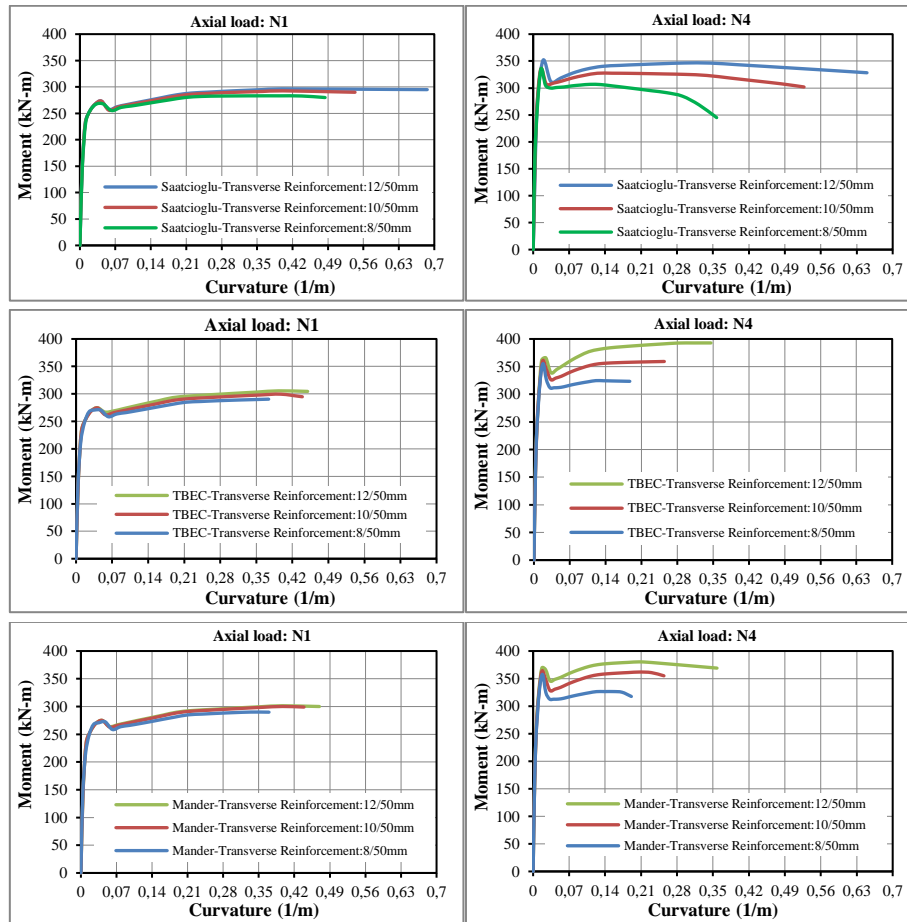


Figure 9. Moment-curvature relationships for different transverse reinforcement diameter and axial load levels.

### 6. RESEARCH FINDINGS AND DISCUSSION

Results obtained for RC column models according to confined concrete models for the different parameters are presented comparatively. A comparison of effective lateral confining pressure ( $f'_l, f_l, \sigma_{2e}$ ) obtained for different parameters are given in Fig. 10. Comparisons of the ratio of the confined to unconfined concrete strength

( $f'_{cc}$  and  $f_{cc}$ ) obtained for different parameters are given in Fig. 11. A comparison of strain at maximum compressive stress ( $\epsilon_{cc}, \epsilon_{c0c}$ ) and maximum compressive strain ( $\epsilon_{cu}, \epsilon_{c20}$ ) of confined concrete obtained for different parameters are given in Fig. 12 and Fig. 13, respectively.

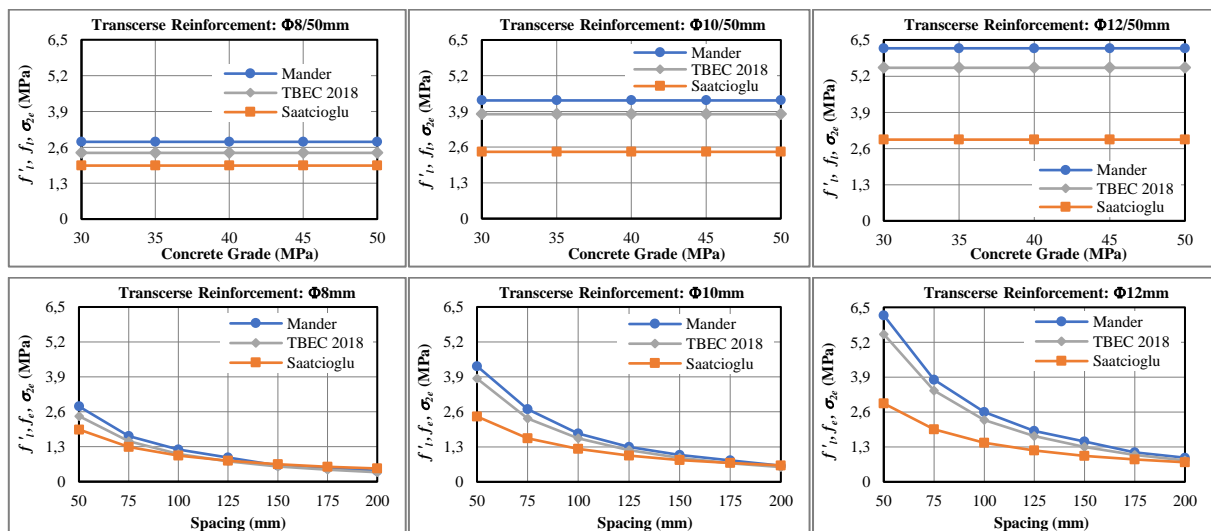


Figure 10. Comparison of  $f'_l, f_l$  and  $\sigma_{2e}$  obtained for different concrete grade and transverse reinforcement spacing.

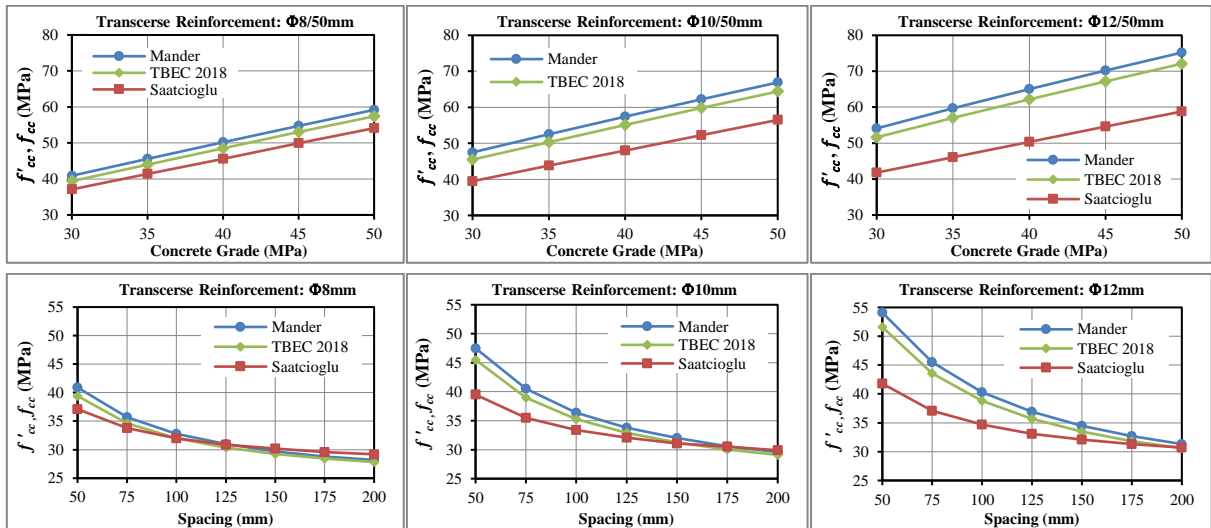


Figure 11. Comparison of  $f'_{cc}$  and  $f_{cc}$  obtained for different concrete grade and transverse reinforcement spacing

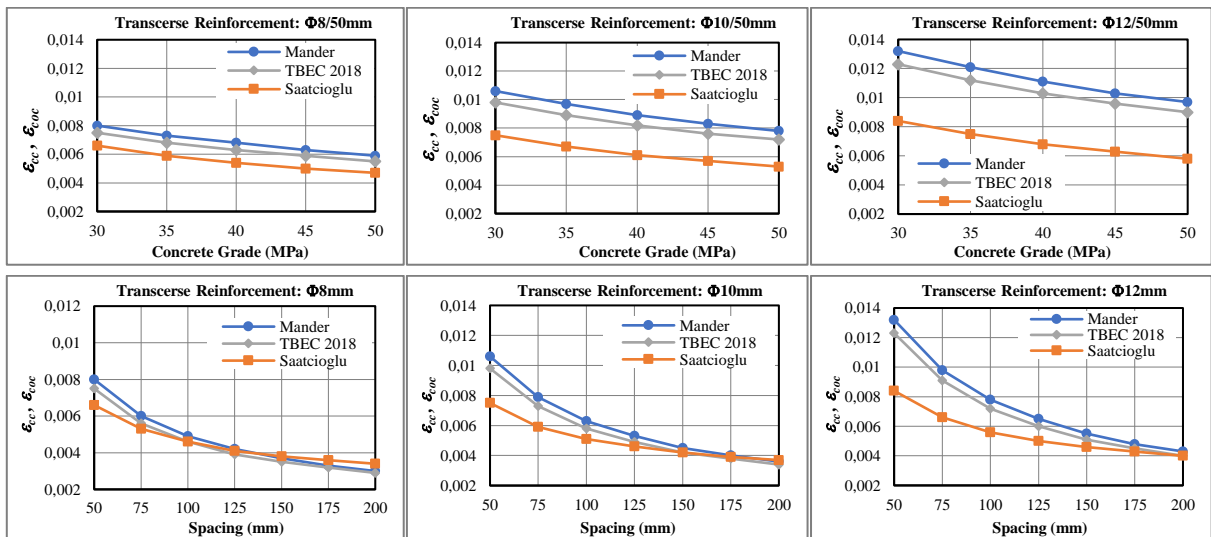


Figure 12. Comparison of  $\epsilon_{cc}$  and  $\epsilon_{coc}$  obtained for different concrete grade and transverse reinforcement spacing

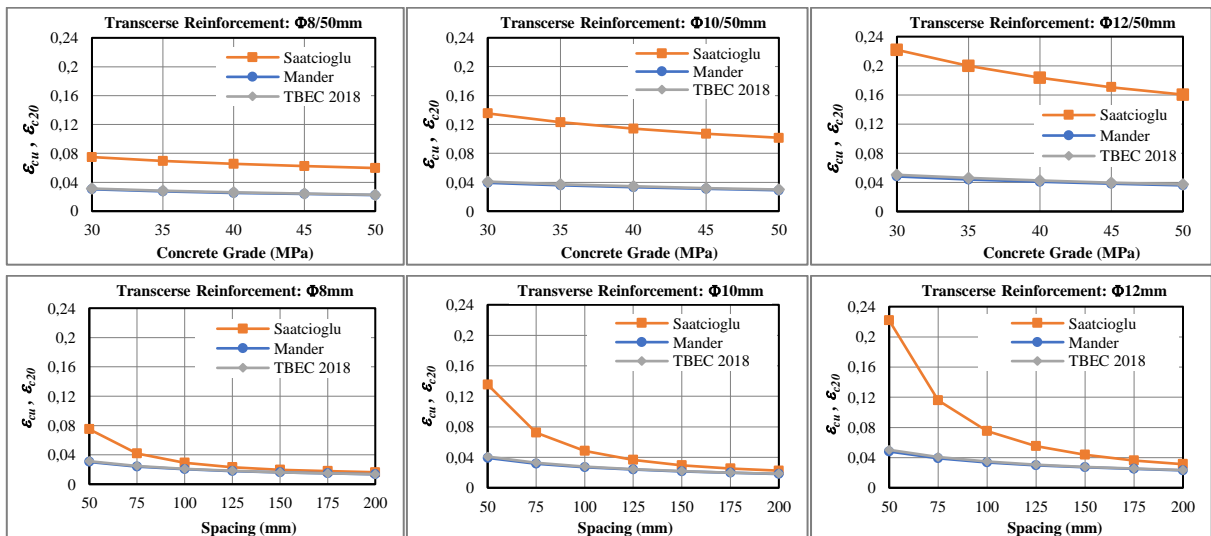


Figure 13. Comparison of  $\epsilon_{cu}$  and  $\epsilon_{c20}$  obtained for different concrete grade and transverse reinforcement spacing.

It was observed that for all models, the transverse reinforcement ratio have an effect on the bearing capacity and ductility of the concrete cross-section. In all three confined concrete models; with increasing transverse reinforcement spacing, confined concrete compressive strength, corresponding strain at maximum concrete stress and maximum concrete compressive strain values for confined concrete decreases. Confined concrete compressive strength, corresponding strain at maximum concrete stress and maximum concrete compressive strain values for confined concrete increase with increasing diameter of the transverse reinforcement. Confined concrete compressive strength values increase with the increasing concrete grade in RC column models. Corresponding strain at maximum concrete stress and maximum concrete compressive strain values for confined concrete decrease according to the increasing concrete class. The effective lateral confining stress value increases with increasing transverse reinforcement diameter, but decreasing with increasing transverse reinforcement spacing. Effective lateral confining stress value remains constant with increasing concrete grade. According to TBEC and Mander models, confinement effectiveness coefficient values increase with increasing transverse reinforcement diameter but decreasing with increasing transverse reinforcement spacing. According to the Saatcioglu and Ravzi model, the confinement effectiveness coefficient value decreases with the increase of the transverse reinforcement diameter and remains constant with the increase of the transverse reinforcement spacing. The confinement effectiveness coefficient values do not change with the increasing concrete grade in all three models. In the RC column models designed, small differences were observed between the maximum compressive strain for confined concrete values calculated from TBEC and Mander for different parameters. Compared to Saatcioglu and Ravzi model, higher maximum compressive strain for confined concrete value is obtained. According to the analysis results obtained, the differences between TBEC and Mander model are less than the Saatcioglu and Ravzi model. For the minimum transverse reinforcement space, the calculated confined concrete strength in the Mander model is higher than the confined concrete strength in

Saatcioglu and Ravzi models. With the increase in the transverse reinforcement spacing and the decrease in the differences of confined concrete strength, approximately Equational strength is obtained. As a result, it has been observed that when transverse reinforcement is close to minimum and minimum spacing value, high confined concrete strength is obtained from the Mander model than Saatcioglu and Ravzi model.

The differences between the ultimate moment and curvature values calculated according to TBEC, Mander, Saatcioglu and Ravzi models were obtained using the Eqs. (15, 16, 17 and 18). The deviation (D%) of analysis results relative to the different confined concrete models were calculated as in Eqs. (15, 16, 17 and 18) and the results are presented in Table 2 and 3. In strain-strain relations, the largest strain value was calculated in the Saatcioglu and Ravzi models. In the moment-curvature relations, the greatest curvature values were obtained in the Saatcioglu and Ravzi models. Curvature values obtained from the analysis results in the deviation (D%) of Saatcioglu and Ravzi relative to the TBEC and Mander model analysis result was calculated. Confined concrete compressive strength was calculated more than other models in Mander model. However, with the increase of the transverse reinforcement spacing for the minimum transverse reinforcement diameter, great value is obtained in the Saatcioglu and Ravzi model. Confined concrete compressive strength obtained from Mander model with the increase of the transverse reinforcement diameter is higher than other models. Moment values obtained from the analysis results in the deviation (D%) of Mander model relative to the TBEC and Saatcioglu and Ravzi analysis result was calculated.

$$D\% = \left[ \frac{\text{Saatcioglu and Ravzi (1992)} - \text{Mander (1988)}}{\text{Saatcioglu and Ravzi (1992)}} \right] \quad (15)$$

$$D\% = \left[ \frac{\text{Saatcioglu and Ravzi (1992)} - \text{TBEC (2018)}}{\text{Saatcioglu and Ravzi (1992)}} \right] \quad (16)$$

$$D\% = \left[ \frac{\text{Mander (1988)} - \text{TBEC (2018)}}{\text{Mander (1988)}} \right] \quad (17)$$

$$D\% = \left[ \frac{\text{Mander (1988)} - \text{Saatcioglu and Ravzi (1992)}}{\text{Mander (1988)}} \right] \quad (18)$$

**Table 2.** Comparison of the ultimate moment and curvature values calculated according to different models for confined concrete for different transverse reinforcement diameter.

Transverse reinforcement: Φ8/50mm										
Axial Load	Models for confined concrete					Deviation (D%) of analysis results				
	Mander et al (1988)	TBEC (2018)		Saatcioglu and Ravzi (1992)		Eq. (15)	Eq. (16)	Eq. (17)	Eq. (18)	
	$C_u$	$M_u$	$C_u$	$M_u$	$C_u$	$M_u$	$C_u$	$M_u$		
N1	0.374	290.4	0.370	290.0	0.464	283.3	19.40	20.26	0.14	2.44
N4	0.191	357.5	0.187	355.4	0.357	335.8	46.50	47.62	0.59	6.07
Transverse reinforcement: Φ10/50mm										
N1	0.445	300.1	0.439	299.5	0.5734	292.7	22.39	23.44	0.20	2.47
N4	0.260	363.4	0.255	360.4	0.5274	333.8	50.70	51.65	0.83	8.15
Transverse reinforcement: Φ12/50mm										
N1	0.458	305.3	0.450	301.5	0.686	296.4	33.24	34.40	1.24	2.92
N4	0.271	392.8	0.266	382.8	0.650	351.5	58.31	59.08	2.55	10.51

**Table 3.** Comparison of the ultimate moment and curvature values calculated according to different concrete models for different transverse reinforcement spacing and axial load levels.

Transverse reinforcement: $\Phi 8/50\text{mm}$										
Axial Load	Models for confined concrete						Deviation (D%) of analysis results			
	Mander et al (1988)		TBEC (2018)		Saatcioglu and Ravzi (1992)		Eq. (15)	Eq. (16)	Eq. (17)	Eq. (18)
	$C_u$	$M_u$	$C_u$	$M_u$	$C_u$	$M_u$	$C_u$		$M_u$	
N1	0.374	290.4	0.37	290.0	0.464	283.3	19.40	20.26	0.14	2.44
N2	0.258	318.0	0.255	316.6	0.449	310.1	42.54	43.21	0.44	2.48
N3	0.207	337.5	0.202	335.8	0.38	328.1	45.53	46.84	0.50	2.79
N4	0.191	357.5	0.187	355.4	0.357	335.8	46.50	47.62	0.59	6.07
Transverse reinforcement: $\Phi 8/75\text{mm}$										
N1	0.275	279.5	0.27	278.4	0.337	272.9	18.40	19.88	0.39	2.36
N2	0.187	312.2	0.183	310.9	0.260	304.7	28.08	29.62	0.42	2.40
N3	0.167	334.7	0.163	333.1	0.244	326.5	31.56	33.20	0.48	2.45
N4	0.142	352.9	0.138	350.2	0.211	338.9	32.70	34.60	0.77	3.97
Transverse reinforcement: $\Phi 8/100\text{mm}$										
N1	0.224	274.0	0.219	272.4	0.253	270.4	11.46	13.44	0.58	1.31
N2	0.152	312.0	0.148	309.8	0.183	303.0	16.94	19.13	0.71	2.88
N3	0.138	334.4	0.134	332.1	0.167	324.4	17.37	19.76	0.69	2.99
N4	0.112	349.2	0.1085	347.0	0.139	337.3	19.42	21.94	0.63	3.41
Transverse reinforcement: $\Phi 8/125\text{mm}$										
N1	0.183	272.8	0.178	271.1	0.192	270.7	4.69	7.29	0.62	0.77
N2	0.136	310.3	0.132	308.2	0.144	303.3	5.56	8.33	0.68	2.26
N3	0.122	334.1	0.118	331.0	0.135	326.2	9.63	12.59	0.93	2.36
N4	0.105	345.2	0.101	341.6	0.122	336.1	13.93	17.21	1.04	2.64
Transverse reinforcement: $\Phi 8/150\text{mm}$										
N1	0.170	271.3	0.164	270.1	0.178	270.0	4.49	7.87	0.44	0.48
N2	0.133	309.5	0.127	308.0	0.143	304.5	6.99	11.19	0.48	1.62
N3	0.110	330.1	0.104	327.5	0.125	324.2	12.00	16.80	0.79	1.79
N4	0.084	343.6	0.079	339.9	0.102	335.3	17.65	22.55	1.08	2.42
Transverse reinforcement: $\Phi 8/175\text{mm}$										
N1	0.144	270.8	0.137	269.8	0.136	270.3	-5.88	-0.74	0.37	0.18
N2	0.118	308.5	0.112	307.1	0.109	305.4	-8.26	-2.75	0.45	1.00
N3	0.101	329.2	0.095	327.4	0.092	325.0	-9.78	-3.26	0.55	1.28
N4	0.080	342.00	0.075	339.1	0.067	334.4	-19.40	-11.94	0.85	2.22
Transverse reinforcement: $\Phi 8/200\text{mm}$										
N1	0.139	270.1	0.135	268.6	0.12	269.4	-15.83	-12.50	0.56	0.26
N2	0.109	308.1	0.105	307.0	0.101	305.1	-7.92	-3.96	0.36	0.97
N3	0.096	328.2	0.087	327.2	0.081	323.7	-18.52	-7.41	0.30	1.37
N4	0.077	338	0.069	337.5	0.064	333.6	-20.31	-7.81	0.15	1.30

As can be seen from the examination of ultimate curvature values calculated for different transverse reinforcement diameter; the greater values are calculated from the Saatcioglu and Ravzi models as %25 for the  $N/N_{max} = 0.10$  level and %52 for the  $N/N_{max} = 0.40$  level compared to the Mander model. As can be seen from the examination of ultimate curvature values calculated for different transverse reinforcement diameter; a higher value is calculated from the Saatcioglu and Ravzi models as %26 for the  $N/N_{max} = 0.10$  level and %53 for the  $N/N_{max} = 0.40$  level compared to TBEC. As can be seen from the examination of ultimate moment values calculated for different transverse reinforcement diameter; the greater value is calculated from the Mander model as %2.6 for the  $N/N_{max} = 0.10$  level and %8.2 for the  $N/N_{max} = 0.40$  level compared to the Saatcioglu and Ravzi model. As can be seen from

the examination of ultimate moment values calculated for different transverse reinforcement diameter; a higher value is calculated from the Mander model as %0.5 for the  $N/N_{max} = 0.10$  level and %1.3 for the  $N/N_{max} = 0.40$  level compared to TBEC.

As can be seen from the examination of ultimate curvature values calculated for fixed transverse reinforcement diameter, different transverse reinforcement spacing and axial load levels; the values calculated from the Saatcioglu and Ravzi model for the 50mm transverse reinforcement spacing was %38 greater than the Mander model and %39 greater than TBEC. The values calculated from the Saatcioglu and Ravzi model for the 75mm transverse reinforcement spacing is %28 greater than the Mander model and %29 greater than TBEC. The value calculated from the Saatcioglu and Ravzi model for the 100mm transverse reinforcement

spacing is %16 higher than the Mander model and %19 greater than the TBEC. The value calculated from the Saatcioglu and Ravzi model for the 125mm transverse reinforcement spacing is %10 higher than the Mander model and %15 greater than the TBEC. The values calculated from the Saatcioglu and Ravzi model for the 150mm transverse reinforcement spacing is %8 higher than the Mander model and %11 greater than TBEC. The value calculated from the Saatcioglu and Ravzi models for the 175mm transverse reinforcement spacing is %11 lower than the Mander model and %5 smaller than TBEC. The value calculated from the Saatcioglu and Ravzi model for the 200mm transverse reinforcement spacing was %16 smaller than the Mander model and %8 smaller than TBEC.

As can be seen from the examination of ultimate moment values calculated for fixed transverse reinforcement diameter, different transverse reinforcement spacing and axial load levels; the values calculated from the Mander model for the 50mm transverse reinforcement spacing was %3.4 greater than the Saatcioglu and Ravzi model and %0.4 greater than TBEC. The value calculated from the Mander model for the 75mm transverse reinforcement spacing is %2.8 greater than the Saatcioglu and Ravzi model and %0.5 greater than TBEC. The value calculated from the Mander model for the 100mm transverse reinforcement spacing is %2.6 higher than the Saatcioglu and Ravzi model and %0.8 greater than the TBEC. The value calculated from the Mander model for the 125mm transverse reinforcement spacing is %2 higher than the Saatcioglu and Ravzi model and %0.7 greater than the TBEC. The value calculated from the Mander model for the 150mm transverse reinforcement spacing is %1.6 higher than the Saatcioglu and Ravzi model and %0.7 greater than TBEC. The value calculated from the Mander model for the 175mm transverse reinforcement spacing is %1.2 higher than the Saatcioglu and Ravzi model and %0.6 greater than TBEC. The value calculated from the Mander model for the 200mm transverse reinforcement spacing is %1.1 higher than the Saatcioglu and Ravzi model and %0.3 greater than TBEC. In the research findings and discussion section, the percentage values obtained from the comparison results of different models are given on average.

When the results obtained from the study are analyzed, it has been observed that there are different results in the cross-section moment and curvature values calculated according to Saatcioglu and Ravzi, Mander and TBEC models. It is observed that the variation of the axial load and transverse reinforcement ratio have an important effect on the moment-curvature behavior of the RC square columns. With increasing axial loads ultimate moment values increase, however, the ultimate curvature values decrease. The cross-section ductility decreases when the transverse reinforcement spacing is increased under constant axial load. As can be seen from the moment-curvature relationships, it is observed that the cross-section ductility and the curvature increase significantly with the reduction of the transverse

reinforcement spacing. The ratio of transverse reinforcement is effective in the cross-section behavior of the RC cross-section. The increase in transverse reinforcement diameter increases the ductility of the cross-section and the maximum moment bearing capacity. The increase in the transverse reinforcement diameter increases the ultimate moment and ultimate curvature values. With the increase of the transverse reinforcement ratio, more ductile behavior is achieved due to the increment of curvature ductility on RC columns.

## 7. CONCLUSION

It has been found that for all models, transverse reinforcement ratio are effective on the lateral load-bearing capacity. The transverse reinforcement spacing densification has a greater effect on the ductility and the bearing capacity of a column cross-section. The increase of the transverse reinforcement ratio increases the ductility and the maximum bearing capacity of a column cross-section. The result is that the axial load is a very important parameter affecting the ductility of the column cross-section. The relationship between axial load and ductile behavior is generally inversely proportional. The increase in the axial load level causes the curvature values to decrease, although it usually increases the moment capacity of the column cross-section. As the diameter of the transverse reinforcement increases, the moment capacity of the column cross-section increases as expected. The effect of axial load on cross-sectional behavior appears to be more explicit in cross-sections where the transverse reinforcement spacing is minimum. If the analysis results are compared the ultimate moment capacities of the sections increase when the decrease of the transverse reinforcement spacing. Moreover, the more ductile behavior for RC cross-sections is observed due to increment of curvature ductility on RC square columns with the increase of transverse reinforcing ratio.

As can be seen from the examination of the moment-curvature relationships obtained according to the confined concrete models, the greatest ultimate curvature values were calculated from the Saatcioglu and Ravzi models (average 24%, the Saatcioglu model is larger). This is a natural result because the greatest strain value in stress-strain relations is also obtained in the Saatcioglu and Ravzi models. This is because Saatcioglu and Ravzi model is directly formed by a rising parabolic arm, a linearly falling arm up to 20% of the strength, and a stable continuation after that point. As can be seen from the examination of ultimate curvature values obtained according to the Mander model and TBEC, there is not much difference (average 3.5% mander model is larger). There is a negligible difference between the ultimate moment values obtained according to the Mander model and TBEC. It is seen from the results of the analysis that there is not much difference between the stress and strain values obtained for these two models. According to Mander, Saatcioglu and Ravzi models, the average

difference value is 3.1% between the ultimate moment values. With the increase in the transverse reinforcement spacing and the decrease in the differences of the ultimate moment values, approximately Equational strength is obtained. As a result, it has been observed that when the close to minimum and minimum spacing value, high confined concrete strength values and the ultimate moment values are obtained from the Mander model than Saatcioglu and Ravzi model. These differences are not much between the Mander model and TBEC.

#### ACKNOWLEDGEMENT

The authors thank the reviewers who evaluated the article for their time and valuable comments and suggestions.

#### DECLARATION OF ETHICAL STANDARDS

The authors of this article declare that the materials and methods used in this study do not require ethical committee permission and/or legal-special permission.

#### CONFLICT OF INTEREST

There is no conflict of interest in this study.

#### AUTHORS' CONTRIBUTIONS

**Saeid FOROUGHİ:** The analysis plan for the study, the design of the reinforced concrete column models, the data collection, analysis, evaluation of the results and the writing of the article.

**Süleyman Bahadır YÜKSEL:** The analysis plan for the study, the design of the reinforced concrete column models and analyzed the numerical results in terms of absolute error.

#### REFERENCES

- [1] Ucar T., Merter O. and Duzgun M., "Determination of lateral strength and ductility characteristics of existing mid-rise RC buildings in Turkey", *Computers and Concrete*, 16(3), 467-485, (2015).
- [2] Yuksel S.B. and Foroughi S., "Analytical Investigation of Confined and Unconfined Concrete Strength of RC Columns", *Konya Journal of Engineering Sciences*, 7(3), 612-631, (2019).
- [3] Foroughi S. and Yuksel S.B., "Investigation of the Moment-Curvature Relationship for RC Square Columns", *Turkish Journal of Engineering (TUJE)*, 4(1), 36-46, (2020).
- [4] Foroughi S., Jamal R. and Yuksel S.B., "Effect of Confining Reinforcement and Axial Load Level on Curvature Ductility and Effective Stiffness of Reinforced Concrete Columns", *El-Cezeri Journal of Science and Engineering*, 7(3), 1309-1319, (2020).
- [5] Foroughi S. and Yuksel S.B., "Analytical investigation of curvature ductility of reinforced concrete columns", *Uludağ University Journal of The Faculty of Engineering*, 25(1), 27-38, (2020).
- [6] Yuksel S.B. and Foroughi S., "Analysis of Bending Moment-Curvature and the Damage Limits of Reinforced Concrete Circular Columns", *Avrupa Bilim ve Teknoloji Dergisi*, (19), 891-903, (2020).
- [7] Olivia M. and Mandal P., "Curvature Ductility Factor of Rectangular Sections RC Beams", *Journal of Civil Engineering*, 16(1), 1-13, (2005).
- [8] Ćurić I., Radić J. and Franetović M., "Determination of the Bending Moment-Curvature Relationship for RC Hollow Section Bridge Columns", *Tehnicki Vjesnik - Technical Gazette*, 23(3), 907-915, (2016).
- [9] Dok G., Ozturk H. and Demir A., "Determining Moment-Curvature Relationship of RC Columns", *The Eurasia Proceedings of Science, Technology, Engineering and Mathematics*, 1, 52-58, (2017).
- [10] Bedirhanoglu I. and Ilki A., "Theoretical Moment-Curvature Relationships for RC Members and Comparison with Experimental Data", *Sixth International Congress on Advances in Civil Engineering*, 6-8 October Bogazici University, Istanbul, Turkey, pp. 231-240, (2004).
- [11] Jun J. and Hui W., "The Relationship between Moment and Curvature and the Elastic-Plastic Seismic Response Analysis of High Pier Section", *the Open Mechanical Engineering Journal*, 9, 892-899, (2015).
- [12] Milašinović D.D., Goleš D. and Ceh A., "Rheological-Dynamical Continuum Damage Model Applied to Research of the Rotational Capacity of a Reinforced Concrete Beams", *Periodica Polytechnica Civil Engineering*, 60(4), 661-667, (2016).
- [13] Milasinovic D.D. and Goles D., "Geometric Nonlinear Analysis of Reinforced Concrete Folded Plate Structures by the Harmonic Coupled Finite Strip Method", *Periodica Polytechnica Civil Engineering*, 58(3), 173-185, (2014).
- [14] Haytham F., Isleem H.F., Wang, D. and Wang, Z., "No Access Axial stress-strain model for square concrete columns internally confined with GFRP hoops", *Magazine of Concrete Research*, 70(20), 1064-1079, (2018).
- [15] Dong C.X., Kwan A.K.H. and Ho J.C.M., "Effects of confining stiffness and rupture strain on performance of FRP confined concrete", *Engineering Structures*, 97, 1-14, (2015).
- [16] Binici B., "An analytical model for stress-strain behavior of confined concrete", *Engineering Structures*, 27(7), 1040-1051, (2005).
- [17] Colajanni P., Papia M. and Spinella N., "Stress-Strain Law for Confined Concrete with Hardening or Softening Behavior", *Hindawi Publishing Corporation, Advances in Civil Engineering*, Volume 2013, Article ID 804904, 11,(2013).
- [18] TBEC, *Turkish Building Earthquake Code*, Specification for Buildings to be Built in Seismic Zones, Ministry of Public Works and Settlement Government of the Republic of Turkey, (2018).
- [19] Mander J.B., Priestley M.J.N. and Park R., "Theoretical stress-strain model for confined concrete", *Journal of Structural Engineering, ASCE*, 114 (8), 1804-26, (1988).

- [20] Saatcioglu M. and Ravzi S.R., “Strength and ductility of confined concrete”, *Journal of Structural Engineering*, 118(6), 1590-1607, (1992).
- [21] SAP2000, Structural Software for Analysis and Design, Computers and Structures, Inc, USA.
- [22] Won D.H., Han T.H., Kim S., Lee J.H. and Kang Y.J., “Confining Effect of Concrete in Double-Skinned Composite Tubular Columns”, *Computers and Concrete*, 14(5), 613-633, (2014).
- [23] Song Z. and Lu Y., “Numerical Simulation of Concrete Confined by Transverse Reinforcement”, *Computers and Concrete*, 8(1), 23-41, (2011).
- [24] Nematzadeh M. and Haghinejad A., “Analysis of Actively-Confined Concrete Columns Using Prestressed Steel Tubes”, *Computers and Concrete*, 19(5), 477-488, (2017).
- [25] Popovics S., “A numerical approach to the complete stress-strain curves for concrete”, *Cement and Concrete Research*, 3(5), 583-599, (1973).
- [26] ACI318., “Building code requationuirements for RC and commentary”, *American Concrete Institute Committee*, ISBN: 978-0-87031-930-3. (2014).